The results presented above support the idea that expansion of TCR $V_\beta 8^+$ encephalitogenic T cells during EAE induces a regulatory network directed in part at the TCR-V_β8-39-59 peptide. The ability of this TCR peptide to trigger a natural regulatory network and to produce a beneficial therapeutic effect is a step forward in the quest to manipulate selective T cell responses to autoantigens in established disease. The rapid therapeutic effect of the TCR peptide is reminiscent of passive TCR antibody therapy reported in the mouse and rat models of EAE (*1, 12, 13*). However, the TCR peptide would have several advantages over passive antibody therapy, including its lack of foreign antigenic determinants and its ability to trigger long-lasting natural regulatory mechanisms. In addition, the ability to treat EAE with an id or subcutaneous injection of peptide in saline (without adjuvants) provides a feasible route for the eventual treatment of humans.

Of equal importance is the demonstration that the regulatory network directed at the synthetic TCR peptide is induced as a consequence of the autoimmune disease itself. By implication, the mere presence of a given anti-TCR response in patients with autoimmune disease would indicate its importance as a target of the immune network that potentially could be triggered with clinical benefit by injecting small doses of the appropriate soluble TCR peptide. T cells from patients with multiple sclerosis, in which BP may be a relevant target autoantigen, use a limited set of V region genes in plaque tissue (*14*) and in response to human myelin basic protein (*15, 16*). Our data would predict increased anti-idiotypic responses to the overexpressed TCR V genes if the T cells were involved in the pathogenesis of the disease, but no detectable or amplifiable responses if the T cells represent a baseline frequency. The presence of anti-TCR responses in vitro would thus provide the impetus for periodic TCR peptide therapy to boost and maintain specific anti-idiotypic responses in patients with established autoimmune disease.

The V_β8-39-59 peptide may not be the only important determinant on T cells (*17–21*) or the TCR (*8*), however, because other sequences within the TCR α or β chains may also induce regulatory T cells and antibodies. Our data do not distinguish the relative importance of immunity directed at this TCR peptide with respect to other well-described regulatory mechanisms, such as suppressor circuits (*22–26*) or cytotoxic T cells (*27–28*) directed at determinants on encephalitogenic effector cells. However, it is clear from its protective, suppressive, and therapeutic effects that the TCR-V_β8-39-59 sequence constitutes an important determinant for the idiotypic regulation of EAE.

REFERENCES AND NOTES

1. H. Acha-Orbea *et al.*, *Cell* **54**, 263 (1988).
2. F. R. Burns *et al.*, *J. Exp. Med.* **169**, 27 (1989).
3. J. Chluba, C. Steeg, A. Becker, H. Wekerle, J. T. Epplen, *Eur. J. Immunol.* **19**, 279 (1989).
4. E. Heber-Katz and H. Acha-Orbea, *Immunol. Today* **10**, 164 (1989).
5. H. Acha-Orbea, L. Steinman, H. O. McDevitt, *Annu. Rev. Immunol.* **7**, 371 (1989).
6. V. Kumar, D. H. Kono, J. L. Urban, L. Hood, *ibid.*, p. 657.
7. A. A. Vandenbark, G. Hashim, H. Offner, *Nature* **341**, 541 (1989).
8. M. D. Howell *et al.*, *Science* **246**, 668 (1989).
9. G. A. Hashim *et al.*, *J. Immunol.* **144**, 4621 (1990).
10. H. Offner, B. A. Standage, D. R. Burger, A. A. Vandenbark, *J. Neuroimmunol.* **9**, 147 (1984).
11. H. Offner *et al.*, *J. Immunol.* **141**, 3828 (1988).
12. J. Urban *et al.*, *Cell* **54**, 577 (1988).
13. M. Owhashi and E. Heber-Katz, *J. Exp. Med.* **168**, 2153 (1988).
14. J. R. Oksenberg *et al.*, *Nature* **345**, 344 (1990).
15. Y. K. Chou *et al.*, *J. Neurosci. Res.*, in press.
16. K. W. Wucherpfennig *et al.*, *Science* **248**, 1016 (1990).
17. G. A. Hashim, *Neurochem. Res.* **6**, 699 (1981).
18. A. Ben-Nun and I. R. Cohen, *Eur. J. Immunol.* **11**, 195 (1981).
19. O. Lider, T. Reshef, E. Beraud, A. Ben-Nun, I. R. Cohen, *Science* **239**, 181 (1988).
20. H. Offner, R. Jones, B. Celnik, A. A. Vandenbark, *J. Neuroimmunol.* **21**, 13 (1989).
21. A. W. Lohse, F. Mor, N. Karin, I. R. Cohen, *Science* **244**, 820 (1989).
22. C. C. Bernard, *Clin. Exp. Immunol.* **29**, 100 (1977).
23. A. M. Welch, J. H. Holda, R. H. Swanborg, *J. Immunol.* **125**, 186 (1980).
24. W. C. Lyman, C. F. Brosnan, A. S. Kadish, C. S. Raine, *Cell. Immunol.* **85**, 542 (1984).
25. S. Varriale *et al.*, *J. Immunol.* **125**, 186 (1989).
26. R. W. Whitham, A. A. Vandenbark, D. N. Bourdette, Y. K. Chou, H. Offner, *Cell. Immunol.* **126**, 290 (1990).
27. K. E. Ellerman, J. M. Powers, S. W. Brostoff, *Nature* **331**, 265 (1988).
28. D. Sun, U. Qin, J. Chluba, J. T. Epplen, H. Wekerle, *ibid.* **332**, 843 (1988).

29. The authors thank B. Celnik for technical assistance, J. Turner for graphic design, and L. Gustafson for secretarial assistance. This work was supported by grants NS23444, NS23221, and NS21466 from the Department of Health and Human Services, NSF grant BNS-8819483, the XOMA Corporation, and the Department of Veterans Affairs.

9 August 1990; accepted 31 October 1990

Intrinsic Oscillations of Neocortex Generated by Layer 5 Pyramidal Neurons

LAURIE R. SILVA, YAEL AMITAI,* BARRY W. CONNORS†

Rhythmic activity in the neocortex varies with different behavioral and pathological states and in some cases may encode sensory information. However, the neural mechanisms of these oscillations are largely unknown. Many pyramidal neurons in layer 5 of the neocortex showed prolonged, 5- to 12-hertz rhythmic firing patterns at threshold. Rhythmic firing was due to intrinsic membrane properties, sodium conductances were essential for rhythmicity, and calcium-dependent conductances strongly modified rhythmicity. Isolated slices of neocortex generated epochs of 4- to 10-hertz synchronized activity when *N*-methyl-D-aspartate receptor–mediated channels were facilitated. Layer 5 was both necessary and sufficient to produce these synchronized oscillations. Thus, synaptic networks of intrinsically rhythmic neurons in layer 5 may generate or promote certain synchronized oscillations of the neocortex.

SYNCHRONIZED OSCILLATIONS ARE pervasive in the cerebral cortex. Cortical rhythms, as revealed by the electroencephalogram (EEG), vary with behavioral state; their frequencies range from the 4- to 7-Hz theta waves of sleep to the 14- to 60-Hz waves dominant during alertness (*1*). Neuropathological conditions such as epilepsy and coma can elicit distinctive EEG rhythms. Cortical oscillations may encode sensory information (*2, 3*). Despite the prevalence of rhythmic neocortical activity, little is known about its mechanisms. Some cortical oscillations are clearly driven by periodic input from the thalamus (*4*); however, others may arise within the cortex itself, independent of the thalamus (*5, 6*).

Neurons generate rhythms in a variety of ways. Some have an intrinsic propensity to oscillate (*7*), and groups of these may interact synaptically to produce synchronous patterns (*4, 8*). Synchronized rhythms can also arise as an emergent property of a network of neurons that, as individuals, are nonrhythmic (*9*). Neurons in the middle layers of neocortex can initiate some nonrhythmic forms of synchronized activity (*10*). We show here that neurons of layer 5 alone have the intrinsic properties and synaptic connections necessary to generate synchronized oscillations.

Recordings were made from neurons in

Section of Neurobiology, Division of Biology and Medicine, Brown University, Providence, RI 02912.

*Present address: Department of Physiology, Ben-Gurion University of the Negev, Beer-Sheva, Israel.
†To whom correspondence should be addressed.

slices of rat sensorimotor cortex maintained in vitro (*11*). Neurons of layer 5 can generate a variety of intrinsic firing patterns (*12*). When membrane potential was held between about −60 and −65 mV, a majority of neurons in deep layer 5 (59%, n = 146) displayed sustained, rhythmic, 5- to 12-Hz patterns of either single spikes or bursts of spikes (*13*). Rhythmic firing could be induced by a brief trigger (Fig. 1A); a 4-ms intracellular current pulse elicited a rhythmic train of single spikes that lasted about 4 s and then stopped abruptly. The mean basal frequency of 28 such single-spiking rhythmic cells was 7.4 ± 0.6 Hz (all data are presented as mean ± SD). Some of the intrinsically bursting cells of layer 5 generated repetitive, rhythmic bursts at basal interburst frequencies of 5 to 10 Hz (6.2 ± 0.5 Hz, n = 18) (Fig. 1B). Epochs of rhythmic firing (usually 1 to 5 s, but sometimes up to 20 s) could also be triggered by spontaneous or evoked postsynaptic potentials. In contrast, neurons with nonrhythmic firing patterns always responded with a single spike or one brief burst under these conditions. Of the 81 single-spiking cells tested within layer 5, 52% showed rhythmic firing; of the 65 intrinsically bursting neurons tested, 68% could burst rhythmically.

The frequency range of rhythmic cells was tested with long (≥800 ms) depolarizing current steps imposed from the resting membrane potentials (Fig. 1, C and E). One of the rhythmic cells' distinguishing characteristics was a bistable state around firing threshold: these cells either were silent or fired continually at their basal frequency (Fig. 1C). As current intensity was raised, rhythmic firing frequencies increased to 35 Hz or more, yet firing showed little or no adaptation (Fig. 1D) even when stimuli were several seconds long. This characteristic was not found in nonrhythmic neurons, which generated only one spike or a brief burst at threshold and adapted during strong stimuli. The responses of rhythmic bursting cells to step stimuli were complex (Fig. 1E). Basal bursting frequency ranged from 5 to 8 Hz and increased with stimulus intensity to maxima of about 16 Hz. Cells frequently made abrupt transitions from bursting to single-spiking, especially in response to stronger stimuli (Fig. 1, E and F).

This rhythmic behavior was observed in recordings from deep layer 5, but not from layers 2, 3, 4, and 6 (n = 30) (*10–12, 14*). Intracellular injections of the dye biocytin (*15*) revealed that both rhythmic bursting (n = 10) and rhythmic single-spiking cells (n = 9) were pyramidal neurons. Each had a soma and profuse basal dendrites within layer 5 and an apical dendrite that branched repeatedly in layers 1 and upper 2 but infrequently within layers 3 and 4.

Rhythmic firing patterns can be generated by intrinsic membrane currents (*7, 16*) or by synaptic feedback circuitry (*9*). Near firing threshold, rhythmic layer 5 cells often generated 5- to 9-Hz damped, subthreshold oscillations as large as 6 mV (Fig. 2, A and B). Subthreshold oscillations occurred even without preceding action potentials (Fig. 2B). Kynurenic acid (5 mM), which nonspecifically antagonizes glutamate receptors, blocked evoked synaptic responses (*17*) but did not change the rhythmic firing patterns or subthreshold oscillations of single neurons (n = 5). These data suggest the presence of an oscillatory mechanism intrinsic to the membrane of each rhythm-generating neuron.

The ionic mechanisms for intrinsic rhythmicity vary considerably among neurons. Many neurons rely on interactions between voltage-sensitive Ca^{2+} conductances and Ca^{2+}-activated K^+ conductances (*7*), whereas some generate oscillations that are Na^+ conductance–dependent but Ca^{2+} conductance–independent (*18*). The rhythms of neocortical cells were completely abolished by the specific Na^+ channel antagonist tetrodotoxin (n = 5). However, bath application of Co^{2+}, an antagonist of voltage-sensitive Ca^{2+} channels (*19*), also disrupted rhythmicity (n = 6) in complex ways (Fig. 2C). Cobalt initially slowed threshold rhythms by about 2 Hz, then blocked them; at the same time, rhythmic single spikes developed into nonrhythmic bursts or prolonged depolarizing plateaus. The data suggest that the rhythms depend

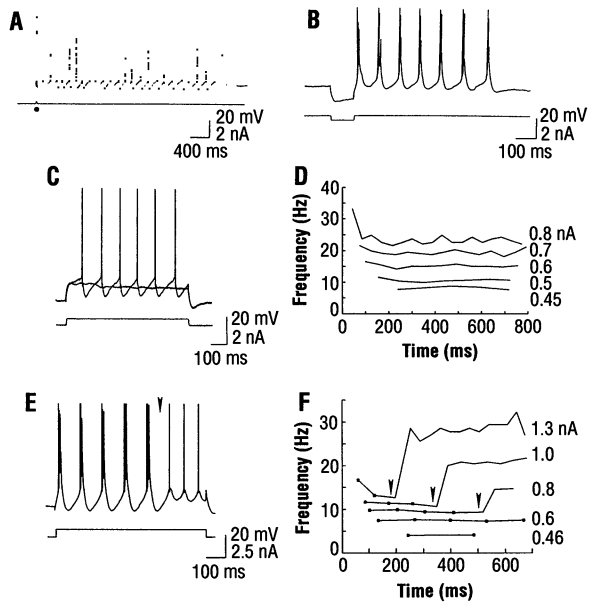

Fig. 1. Rhythmic firing patterns of four neurons from layer 5. (**A**) Rhythmic single-spiking. Baseline membrane potential was depolarized to −60 mV with injected current and a 4-ms depolarizing current pulse (lower trace; dot) evoked a 4-s epoch of spikes with a mean frequency of 6.6 Hz. (**B**) Rhythmic bursting. Baseline potential was −61 mV, and a hyperpolarizing current pulse evoked a seven-burst epoch with a mean interburst frequency of 9.3 Hz. Each burst consisted of three spikes firing at about 150 to 300 Hz. (**C**) Threshold rhythmic response to step depolarizing current. Two consecutive traces superimposed. (**D**) Spiking frequency (estimated as the reciprocal of each interspike interval) as a function of time for various step current intensities. Data are from the cell in (C). (**E**) Response of rhythmic bursting neuron to step current. Current intensity of 0.8 nA generated five consecutive bursts, followed by an abrupt transition to rhythmic single-spiking (arrow). (**F**) Interburst (filled symbols) and single-spike (lines) frequencies as a function of time for various step current intensities. Data are from the cell in (E). (Arrows, transitions from rhythmic bursting to single-spiking).

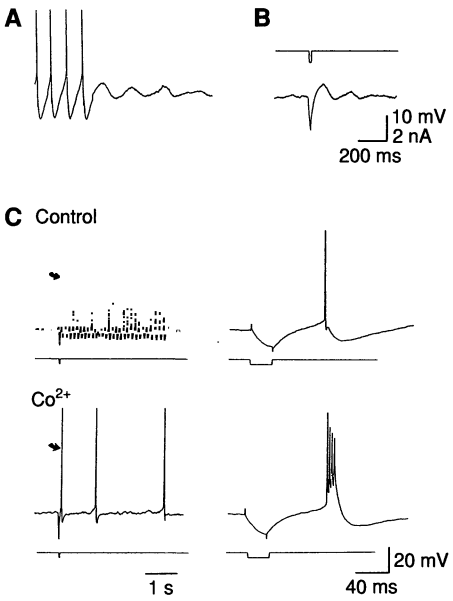

Fig. 2. Rhythmic firing as an intrinsic membrane property of some layer 5 cells. (**A**) Damped oscillation of membrane potential following the end of an evoked rhythmic epoch of single spikes. Membrane potential, −60 mV. (**B**) Damped oscillation of membrane potential following small hyperpolarizing current step. Membrane potential, −62 mV. Calibration in (B) also applies to (A). (**C**) Cobalt disrupts rhythmic firing. Under control conditions (upper left), the cell generated rhythmic epochs of single spikes (8 Hz for 3 s). The first spike (arrow) is shown at higher sweep speed on the right. In the presence of 1.5 mM Co^{2+}, rhythmicity was abolished (lower left). Evoked responses changed to spike bursts. The first spike (arrow) is shown at higher sweep speed on the right.

absolutely on inward Na^+ currents but are also strongly influenced by Ca^{2+} currents. The most important effect of Ca^{2+} influx may be to activate various Ca^{2+}-dependent K^+ currents that terminate slow, Na^+-dependent depolarizations (*20*) and help to set the rhythm frequency.

We explored the possibility that intrinsically rhythmic neurons of layer 5 can generate synchronized cortical oscillations. Some vertebrate nervous systems can produce synchronous rhythms that depend on the *N*-methyl-D-aspartate (NMDA) subtype of glutamate receptor (*21*). Excitatory synapses in neocortex often utilize NMDA receptors (*17, 22*), and reducing the extracellular Mg^{2+} concentration facilitates NMDA-gated currents and causes synchronized discharges in neocortical slices (*23*). We bathed our slices in solutions with (nominally) zero Mg^{2+} concentrations and found that this synchronized activity is highly rhythmic. Field potential recordings in low concentrations of Mg^{2+} consisted of epochs of 4- to 7-Hz waves (Fig. 3A), which were always synchronized across all layers in intact slices. Epochs were typically 1 to 4 s in duration (maximum of 8 s) and recurred spontaneously one to nine times per minute (Fig. 3A, right). These synchronized oscillations were dependent on NMDA receptors, because the specific antagonist 2-amino-5-phosphonovaleric acid (APV) (10 to 50 μM) (*24*) completely blocked them (Fig. 3B). We tested the site of origin of the activity by further dissecting the slices. When they were cut vertically into narrow segments, rhythmic spontaneous activity continued independently in each segment. These segments were then cut horizontally to isolate subsets of layers. Rhythmic activity continued only in those slice fragments that contained layer 5. Fragments that consisted exclusively of layer 5 were also spontaneously rhythmic (Fig. 4). Intracellular recordings showed that pyramidal neurons that had their apical dendrites severed at the border of layers 4 and 5 still generated intrinsic rhythmic firing patterns similar to those in intact cells (n = 6), and that their activity was phase-locked to the rhythmic field potentials when bathed in medium with no Mg^{2+}.

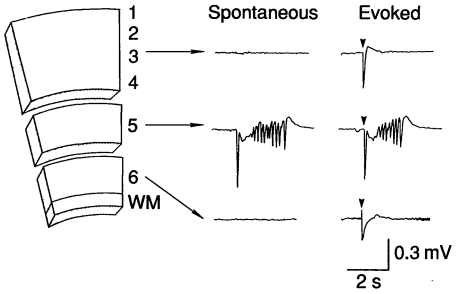

Fig. 4. Sufficiency of layer 5 for synchronized rhythm generation. A slice was preincubated in medium with zero Mg^{2+} concentration, then cut vertically to a maximum width of about 1 mm, at which time all layers displayed synchronized rhythms. Horizontal cuts then trisected the slice at the borders of layers 4 and 5 and layers 5 and 6. Each slice fragment was tested for the presence of spontaneous (left traces) and shock-evoked (right traces) activity. For the two upper fragments, single shocks (arrowheads) were delivered to the lower edges. The layer 6 fragment was shocked at the border of the gray and white matters (WM).

Our results suggest that networks of intrinsically rhythmic neurons in layer 5 can initiate synchronized rhythms and project them on neurons of other layers. Thus, (i) many of the pyramidal neurons of layer 5 had the intrinsic ability to fire in stable, rhythmic patterns at 5 to 12 Hz; (ii) fragments of cortex containing only layer 5 were sufficient to generate synchronized oscillations at 4 to 7 Hz; (iii) fragments of cortex without layer 5 did not oscillate synchronously. The basal frequencies of rhythmic layer 5 cells and NMDA-dependent population rhythms overlap the frequency range of many EEG patterns. Networks of neocortical neurons may be the exclusive pacemakers for some EEG rhythms. Alternatively, the rhythmicity of layer 5 could interact with periodic subcortical input. For example, spindle activity can be generated in the thalamus (*4*), and the resonance of cortical layer 5 would facilitate this. The pacemaker for cortical alpha rhythms (8 to 12 Hz) is unknown, and some evidence suggests they are generated within cortical layers (*25*). High-frequency (20 to 80 Hz) rhythms associated with sensory coding in visual cortex (*3*) may also arise within the cortex (*6*). Although these are faster than the basal rhythms of layer 5 cells, a computational model indicates that neurons with low intrinsic rates of oscillation can, when appropriately coupled synaptically, generate population rhythms of much higher frequencies (*8*).

Our results imply that synchronized rhythmicity in neocortex depends on the tonic activation of NMDA receptors by endogenous glutamate (*26*). NMDA receptors have also been implicated in the synchronized bursts of layer 5 neurons during slow-wave sleep but not during spindles (*27*). It is very likely that the intrinsic rhythmicity of the layer 5 network is modulated by a variety of diffuse neurotransmitter systems (*4, 28*). These could provide a mechanism for switching cortical activity between nonrhythmic and rhythmic modes, as behavioral contingencies demand.

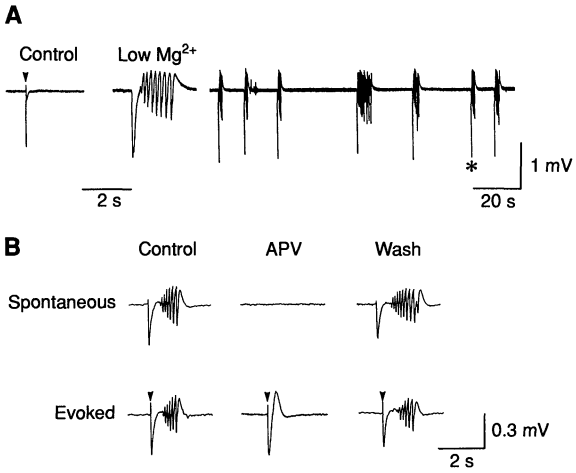

Fig. 3. Synchronized rhythmicity in an intact slice bathed in a solution with nominally zero Mg^{2+} concentration. (**A**) Under control conditions there was no spontaneous field potential activity, but shock (arrow) to deep layers evoked brief, negative deflection (left). After 40- to 50-min wash in medium with zero Mg^{2+} concentration, spontaneous rhythmic potentials were recorded (middle), and these recurred at variable intervals (right). Starred event on the right is shown at high sweep speed in the middle. Left calibration applies to the left and middle traces. (**B**) Both spontaneous and stimulus-evoked (arrows) synchronized rhythms at low Mg^{2+} concentration were reversibly abolished by 10 to 50 μM APV. Monophasic responses could still be evoked in APV (lower, middle), but spontaneous events were absent (upper, middle). All recordings were made from the middle of layers 2 and 3 in intact slices.

REFERENCES AND NOTES

1. K. A. Kooi, R. P. Tucker, R. E. Marshall, *Fundamentals of Electroencephalography* (Harper and Row, Hagerstown, MD, 1978).
2. W. J. Freeman and C. A. Skarda, *Brain Res. Rev.* **10**, 147 (1985).
3. W. J. Freeman and B. W. van Dijk, *Brain Res.* **422**, 627 (1988); R. Eckhorn *et al., Biol. Cybern.* **60**, 121 (1988); C. M. Gray, P. Konig, A. K. Engel, W. Singer, *Nature* **338**, 334 (1989).
4. M. Steriade and R. R. Llinás, *Physiol. Rev.* **68**, 649 (1988).
5. R. Kristiansen and G. Courtois, *EEG Clin. Neurophysiol.* **1**, 265 (1949).
6. C. M. Gray and W. Singer, *Proc. Natl. Acad. Sci. U.S.A.* **86**, 1698 (1989).
7. R. R. Llinás, *Science* **242**, 1654 (1988); Y. Yarom, *Exp. Brain Res.* **17**, 209 (1989).
8. R. D. Traub, R. Miles, R. K. S. Wong, *Science* **243**, 1319 (1989).
9. P. A. Getting, in *Methods in Neuronal Modeling: From Synapses to Networks,* C. Koch and I. Segev, Eds. (MIT Press, Cambridge, MA, 1989), pp. 171–194.
10. M. J. Gutnick, B. W. Connors, D. A. Prince, *J. Neurophysiol.* **48**, 1321 (1982); B. W. Connors, *Nature* **310**, 685 (1984); Y. Chagnac-Amitai and B. W. Connors, *J. Neurophysiol.* **62**, 1149 (1989).
11. The methods have been described [B. W. Connors, R. C. Malenka, L. R. Silva, *J. Physiol. (London)* **406**, 443 (1988)]. Rats were anesthetized with pentobarbital, slices were cut 400 μm thick and superfused with a control solution containing 132 mM NaCl, 3 mM KCl, 2 mM $CaCl_2$, 2 mM $MgSO_4$, 1.25 mM NaH_2PO_4, 26 mM $NaHCO_3$,

10 mM dextrose, saturated with 95% O_2, 5% CO_2, and kept at 34°C. Intracellular microelectrodes were filled with 4 M potassium acetate (80 to 150 megohms); extracellular microelectrodes were filled with 1 M NaCl (about 5 megohms). Cells used for analysis had stable resting potentials ≤ −55 mV and spike heights ≥80 mV. Membrane potential was manipulated with current injected through the electrode. Tetrodotoxin (5 to 10 μM) was applied in droplets to the slice surface via a micropipette.

12. We have recognized three general patterns of intrinsic firing in neocortical cells, regular-spiking (RS), intrinsically bursting (IB), and fast-spiking [reviewed in B. W. Connors and M. J. Gutnick, *Trends Neurosci.* **13**, 99 (1990)]. Diversity of firing patterns among layer 5 RS and IB cells have been observed [D. A. McCormick, B. W. Connors, J. W. Lighthall, D. A. Prince, *J. Neurophysiol.* **54**, 782 (1985); A. Agmon and B. W. Connors, *Neurosci. Lett.* **99**, 137 (1989); Y. Chagnac-Amitai, H. Luhmann, D. A. Prince, *J. Comp. Neurol.* **296**, 598 (1990); A. Mason and A. Larkman, *J. Neurosci.* **10**, 1415 (1990)]. Some of the rhythmic cells described here qualify as IB neurons; others do not easily fit either category since they neither burst nor show the adaptation of RS cells.
13. In a sample of 25 rhythmic neurons from layer 5, both single-spiking and bursting types, the voltage threshold for rhythmic firing was −62 ± 3.5 mV (range of −53 to −67 mV).
14. R. Llinás and A. A. Grace [*Soc. Neurosci. Abstr.* **15**, 660 (1989)] have observed intrinsically rhythmic cells in neocortical layer 4..
15. Biocytin (4%; Molecular Probes, Inc.) was dissolved in the microelectrode filling solution. Tissue was processed with horseradish peroxidase by a modification of the protocol of K. Horikawa and W. E. Armstrong [*J. Neurosci. Methods* **25**, 1 (1988)].
16. B. O. Alving, *J. Gen. Physiol.* **51**, 29 (1968); A. L. F. Gorman and A. Hermann, *J. Physiol. (London)* **333**, 681 (1982).
17. K. A. Jones and R. W. Baughman, *J. Neurosci.* **8**, 3522 (1988).
18. A. Alonso and R. Llinás, *Nature* **342**, 175 (1989).
19. Co^{2+} was substituted for Ca^{2+} at concentrations of 1.0 to 1.5 mM; S. Hagiwara and L. Byerly, *Trends Neurosci.* **6**, 189 (1983); B. Sutor and W. Zieglgänsberger, *Pfluegers Arch.* **410**, 102 (1987).
20. P. C. Schwindt *et al., J. Neurophysiol.* **59**, 424 (1988); P. C. Schwindt, W. J. Spain, W. E. Crill, *ibid.* **61**, 233 (1989).
21. S. Grillner *et al.*, *Trends Neurosci.* **10**, 34 (1987); W. Anderson *et al.*, *Brain Res.* **398**, 215 (1986); P. K. Stanton, R. S. G. Jones, I. Mody, U. Heinemann, *Epilepsy Res.* **1**, 53 (1986).
22. A. M. Thomson, D. C. West, D. Lodge, *Nature* **313**, 479 (1985); B. Sutor and J. J. Hablitz, *J. Neurophysiol.* **61**, 621 (1989).
23. A. M. Thomson, *J. Physiol. (London)* **370**, 531 (1986); E. Hegstad, I. A. Langmoen, J. J. Hablitz, *Epilepsy Res.* **3**, 174 (1989).
24. J. C. Watkins and R. H. Evans, *Annu. Rev. Pharmacol. Toxicol.* **21**, 165 (1981).
25. F. H. Lopes da Silva and W. Storm van Leeuwen, in *Architectonics of the Cerebral Cortex*, M. A. B. Brazier and H. Petsche, Eds. (Raven, New York, 1978), pp. 319–333.
26. J. J. LoTurco, I. Mody, A. R. Kriegstein, *Neurosci. Lett.* **114**, 265 (1990).
27. M. Armstrong-James and K. Fox, *Brain Res.* **451**, 189 (1988).
28. R. A. Nicoll, R. C. Malenka, J. A. Kauer, *Physiol. Rev.* **70**, 513 (1990).
29. We thank L. Cauller for critical comments. Supported by NIH, National Institute of Mental Health, Klingenstein Fund, and McCormick Fund.

21 June 1990; accepted 2 October 1990

A Potent Nonpeptide Antagonist of the Substance P (NK_1) Receptor

R. MICHAEL SNIDER, JAY W. CONSTANTINE, JOHN A. LOWE III, KELLY P. LONGO, WESLEY S. LEBEL, HEIDI A. WOODY, SUSAN E. DROZDA, MANOJ C. DESAI, FREDRIC J. VINICK, ROBIN W. SPENCER, HANS-JÜRGEN HESS

CP-96,345 [(2*S*, 3*S*)-*cis*-2-(diphenylmethyl)-*N*-[(2-methoxyphenyl)-methyl]-1-azabicyclo[2.2.2]octan-3-amine] is a potent nonpeptide antagonist of the substance P (NK_1) receptor. CP-96,345 inhibited ^{3}H-labeled substance P binding and was a classical competitive antagonist in the NK_1 monoreceptor dog carotid artery preparation. CP-96,345 inhibited substance P–induced salivation in the rat, a classical in vivo bioassay, but did not inhibit NK_2, NK_3, or numerous other receptors; it is thus a selective NK_1 antagonist. This compound may prove to be a powerful tool for investigation of the physiological properties of substance P and exploration of its role in diseases.

SUBSTANCE P (SP) (ARG-PRO-LYS-Pro-Gln-Gln-Phe-Phe-Gly-Leu-Met-NH_2) was the first discovered and is the best characterized member of the family of structurally related peptides known as tachykinins (*1*). Additional members sharing the COOH-terminal sequence Phe-X-Gly-Leu-Met-NH_2 (where X is Phe, Tyr, Val, or Ile) of SP include neurokinin A and B and the amphibian peptides physalaemin, eledoisin, and kassinin (*2*). The current nomenclature designates the receptors for SP, neurokinin A, and neurokinin B as NK_1, NK_2, and NK_3, respectively. These peptides and their receptors are widely distributed in the body and are involved in numerous physiological activities (*3–5*), such as vasodilatation (*6*), smooth muscle contraction (*7*), and stimulation of salivary secretion (*8*). There is also considerable evidence supporting a role for SP as a neurotransmitter or neuromodulator, particularly in the transmission of painful stimuli from the periphery and in interactions with other neurotransmitters in the brain (*3, 5, 9*). Substance P also plays a role in the activation of cells of the immune system, including mononuclear leukocytes (monocytes and lymphocytes) and polymorphonuclear leukocytes (*10*).

Studies of the biological effects of these peptides have relied primarily on the ability of agonists to effect contractile responses in tissues that, in many cases, contain more than one type of tachykinin receptor. The characterization of these receptors has been incomplete because of both an overlapping specificity of the peptide agonists and the lack of stable, potent antagonists (*11*). Although peptide antagonists of the SP receptor have been described (*12*), their affinity is several orders of magnitude lower than that of the natural agonist. Moreover, the metabolic instability of peptides limits their usefulness for in vivo studies. We sought, therefore, to discover a nonpeptide SP antagonist.

In the current state of our understanding it is not yet possible to design de novo nonpeptide molecules with high affinity for a macromolecular receptor. Moreover, computer-assisted molecular modeling has not yet produced a high-affinity receptor-active nonpeptide ligand. Accordingly, we used a chemical file–screening approach. The result of this effort was CP-96,345 (Fig. 1) [(2*S*, 3*S*)-*cis*-2-(diphenylmethyl)-*N*-[(2-methoxyphenyl)-methyl]-1-azabicyclo[2.2.2]octan-3-amine] (*13*), a potent inhibitor of [^{3}H]SP binding to bovine caudate membranes. CP-96,345 was virtually equipotent to SP itself in the displacement of [^{3}H]SP from bovine caudate membranes and had a median inhibition concentration (IC_{50} ± SE) of 3.4 ± 0.8 nM (Fig. 2A). In the same assay system, unlabeled SP and the peptide antagonist [D-Pro^2, D-Trp^{7,9}]SP (Folker's peptide), were effective inhibitors of [^{3}H]SP binding, with IC_{50} values of 2.2 ± 0.3 and 2100 ±

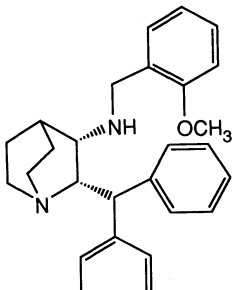

Fig. 1. Structure of CP-96,345.

Department of Exploratory Medicinal Chemistry, Central Research Division, Pfizer Inc., Groton, CT 06340.